Two-fermion Dirac-like eigenstates of the Coulomb QED Hamiltonian

1996 J. Phys. A: Math. Gen. 29 6817

(http://iopscience.iop.org/0305-4470/29/21/015)

J. Phys. A: Math. Gen. **29** (1996) 6817–6841. Printed in the UK

Two-fermion Dirac-like eigenstates of the Coulomb QED Hamiltonian

J W Darewych and L Di Leo

Department of Physics and Astronomy, York University, North York, Ontario M3J 1P3, Canada

Received 10 April 1996, in final form 2 July 1996

Abstract. We point out that the Coulomb part of the QED Hamiltonian in the Coulomb gauge has exact two-fermion eigenstates, provided that the wavefunction satisfies a Dirac-like (or Breit-like) equation. This equation, which describes the relative motion of a system of two fermions of masses m_1 and m_2 and charges q_1 and q_2 interacting via the Coulomb potential, is shown to reduce to the usual Dirac eigenvalue equation when one of m_i is taken to be infinite. For specific J^P states of the two-fermion systems, the equation is reduced to coupled radial equations. Numerical solutions for the mass spectrum $E(\alpha)$ of the two-fermion system as a function of the coupling constant $\alpha = |q_1q_2|/4\pi$ are obtained for $O^{\pm}$ states for various combinations of m_1 and m_2. We find that the ground-state energy of the two-fermion system has normalizable bound-state solutions for $0 \leqslant \alpha \leqslant \alpha_c$, where $\alpha_c = 2$ for $m_1 = m_2$, but decreases towards the one-particle Dirac result of $\alpha_c = 1$ as one of the particle masses tends to infinity. Our numerical results for $E(\alpha)$ are in agreement with conventional perturbative $O(\alpha^4)$ results if $\alpha \ll 1$. Comparison is made with other radial reductions of two-fermion equations with purely Coulombic interactions.

1. Introduction

It has not been possible, to date, to write down exact two-particle eigensolutions of the QED Hamiltonian. However, it is possible to obtain such eigensolutions for a non-trivial portion of it, in the Coulomb gauge. In the present paper we consider eigensolutions for the Coulomb QED Hamiltonian, that is the Hamiltonian of quantum electrodynamics in the Coulomb gauge, but for which the transverse-photon part of the interaction is effectively turned off.

The QED Hamiltonian density for two different fermionic fields $\psi(x)$ and $\phi(x)$, in the Coulomb gauge, can be written as (we use the conventions of [1] with $\hbar = c = 1$):

$$\mathcal{H}_{QED} = \mathcal{H}_\psi + \mathcal{H}_\phi + \mathcal{H}_C + \mathcal{H}_T + \mathcal{H}_\gamma \tag{1}$$

where

$$\mathcal{H}_\psi = \psi^\dagger(x) h_1(x) \psi(x) \tag{2}$$

$$\mathcal{H}_\phi = \phi^\dagger(x) h_2(x) \phi(x) \tag{3}$$

with

$$h_i(x) = -\mathrm{i}\boldsymbol{\alpha} \cdot \boldsymbol{\nabla} + m_i\beta + q_i\phi_c(x) - q_i\boldsymbol{\alpha} \cdot \boldsymbol{A}_c(x) \tag{4}$$

$$\mathcal{H}_C(x) = \frac{1}{8\pi} \int \mathrm{d}^3y \, \frac{\rho(x)\rho(y)}{|\boldsymbol{x} - \boldsymbol{y}|} \tag{5}$$

0305-4470/96/216817+25$19.50

with

$$\rho(x) = q_1\psi^\dagger(x)\psi(x) + q_2\phi^\dagger(x)\phi(x) \tag{6}$$

$$\mathcal{H}_T(x) = -q_1\psi^\dagger(x)\boldsymbol{\alpha}\cdot\boldsymbol{A}(x)\psi(x) - q_2\phi^\dagger(x)\boldsymbol{\alpha}\cdot\boldsymbol{A}(x)\phi(x) \tag{7}$$

and

$$\mathcal{H}_\gamma(x) = \tfrac{1}{2}\dot{\boldsymbol{A}}^2(x) + \tfrac{1}{2}[\boldsymbol{\nabla}\times\boldsymbol{A}(x)]^2. \tag{8}$$

In these equations m_i, q_i ($i = 1, 2$) are the masses and charges associated with the fermionic fields ψ and ϕ, and we have included the possibility that there is also an external classical c-number field, specified by the potential functions ϕ_c, $\boldsymbol{A}_c$. The spinor-field amplitudes ψ, ϕ are, of course, operators in the quantum theory and they satisfy the usual canonical anticommutation relations. The non-vanishing ones are

$$[\psi_\alpha(\boldsymbol{x}, t), \psi^\dagger_\beta(\boldsymbol{y}, t)]_+ = \delta_{\alpha\beta}\delta^3(\boldsymbol{x} - \boldsymbol{y}) \tag{9}$$

$$[\phi_\alpha(\boldsymbol{x}, t), \phi^\dagger_\beta(\boldsymbol{y}, t)]_+ = \delta_{\alpha\beta}\delta^3(\boldsymbol{x} - \boldsymbol{y}) \tag{10}$$

while all others vanish including, in particular,

$$[\psi_\alpha(\boldsymbol{x}, t), \phi^\dagger_\beta(\boldsymbol{y}, t)]_+ = 0. \tag{11}$$

By the Coulomb QED Hamiltonian, H_{CQED}, we mean the one in which the transverse-photon part of the interaction, $\mathcal{H}_T$ of (7) is 'turned off', that is, dropped altogether. This allows one to write down some exact solutions to the resulting field theoretic 'Schrödinger' equation

$$H_{CQED}|f\rangle = E|f\rangle \tag{12}$$

where

$$H_{CQED} = \int \mathrm{d}^3x\, \mathcal{H}_{CQED}(\boldsymbol{x}, t) \tag{13}$$

and

$$\mathcal{H}_{CQED} = \mathcal{H}_\psi + \mathcal{H}_\phi + \mathcal{H}_C. \tag{14}$$

Henceforth, we shall consider the model theory defined by the Hamiltonian (13), which does not contain any dynamical (transverse) photons, that is $\mathcal{H}_T$ is set to zero and $\mathcal{H}_\gamma$ is decoupled. Note that a consequence of the dropping of $\mathcal{H}_T$ is that the resulting model is not covariant.

2. Empty vacuum and one-fermion states

We define an empty vacuum state $|\tilde{0}\rangle$ such that

$$\psi(x)|\tilde{0}\rangle = \phi(x)|\tilde{0}\rangle = 0. \tag{15}$$

Note that $|\tilde{0}\rangle$ is not the usual Dirac vacuum state, $|0\rangle$, of QED, that corresponds to a filled negative-energy sea [1, pp 58–9]. Rather $|\tilde{0}\rangle$, as defined in (15) contains no positive-energy fermions nor a filled sea of negative-energy fermions. The definition (15) means that we are not following the conventional QED approach, in which only the positive frequency part of the spinor-field operators annihilates the Dirac vacuum. Thus, as we show below, we shall be dealing with coordinate space Dirac-like equations, with positive- and negative-energy states, instead of projected momentum-space equations with positive-energy particle and antiparticle states, as happens in the conventional approach. The choice of the unconventional vacuum enables us to write down exact eigensolutions of the Coulomb

QED Hamiltonian, $:H_{CQED}:$. By contrast, in the conventional approach only approximate solutions, primarily perturbative approximations, have been obtained (e.g. [2, 3, 11, 13]). However, the choice of the empty vacuum means that dynamical pair-creation effects (loops), such as vacuum polarization, are not present in this formalism.

Since we shall not be interested here in infinite self-energy questions, we shall work with a normal-ordered form of H_{CQED} in which all our annihilation operators $\psi(x)$ and $\phi(x)$ stand to the right of the creation operators $\psi^\dagger(x)$ and $\phi^\dagger(x)$. This normal ordering is achieved as usual in conformity with all the commutation relations (9)–(11). But we stress that this is not identical to the normal ordering of conventional QED [1, p 60] since ψ, ϕ are not the conventional annihilation operators. Thus, our normal-ordered form of H_C (cf (5)) is

$$:H_C:=\frac{1}{8\pi}\int\frac{\mathrm{d}^3x\,\mathrm{d}^3y}{|\boldsymbol{x}-\boldsymbol{y}|}[q_1^2\psi_\alpha^\dagger(x)\psi_\beta^\dagger(y)\psi_\beta(y)\psi_\alpha(x)+q_1q_2\psi_\alpha^\dagger(x)\phi_\beta^\dagger(y)\phi_\beta(y)\psi_\alpha(x)$$
$$+q_2q_1\phi_\alpha^\dagger(x)\psi_\beta^\dagger(y)\psi_\beta(y)\phi_\alpha(x)+q_2^2\phi_\alpha^\dagger(x)\phi_\beta^\dagger(y)\phi_\beta(y)\phi_\alpha(x)] \tag{16}$$

where $\alpha, \beta = 1, 2, 3, 4$ and summation on repeated indices is implied.

With the above conventions, we note that the state

$$|1\rangle=\int\mathrm{d}^3x\,F_\alpha(\boldsymbol{x})\psi_\alpha^\dagger(x)|\tilde{0}\rangle \tag{17}$$

is an eigenstate of $:H_{CQED}:$ with eigenenergy E_1, provided that the four coefficient amplitudes $F_\alpha(\boldsymbol{x})$ are solutions of

$$\{[h_1(\boldsymbol{x})]_{\alpha\beta}-E_1\delta_{\alpha\beta}\}F_\beta(\boldsymbol{x})=0 \tag{18}$$

or

$$(h_1(\boldsymbol{x})-E_1)F(\boldsymbol{x})=0 \tag{19}$$

in matrix notation, that is provided the spinor F is a solution of the usual Dirac eigenvalue equation (19). We see, therefore, that the exact one-fermion eigenstate (17) leads to the usual Dirac equation with all its well known negative energy 'pathologies'. That is, (18) or (19) has positive-energy solutions with $E = m_1 + \cdots$ as well as negative-energy solutions with $E_1 = -m_1 + \cdots$. We shall refer to $|1\rangle$ as a one-Dirac-particle eigenstate, to $\psi^\dagger(x)$ as a Dirac-particle creation operator, and to $\psi(x)$ as the corresponding annihilation operator. By 'Dirac particle' we mean a particle state described by the full four-component spinor solution $F(\boldsymbol{x})$ of the Dirac equation (19).

In the conventional approach no exact eigensolutions of $:H_{CQED}:$ analogous to the simple form (17)–(19) are possible. The exact solution of the Coulomb problem in the conventional approach involves an infinite chain of Fock states containing any number of particle–antiparticle pairs (e.g. (22) of [22]). In practice, this chain must be truncated at some finite order to allow for tractable solutions. Hardekopf and Sucher [2a], for example, discuss such a lowest-order ('no pair') momentum-space equation. They point out that its ground-state eigenenergy, which for small values of the coupling constant α has the form $E = m(1 - \frac{1}{2}\alpha^2 - \frac{1}{8}\alpha^4 + \cdots)$, agrees with the exact solution $E = \sqrt{1-\alpha^2}$ of the Dirac–Coulomb equation to $\mathrm{O}(\alpha^4)$, but not beyond. More generally, Guiasu and Koniuk [22] have demonstrated that the well known solutions of the Dirac equation are the exact solutions of the one-fermion Coulomb problem in conventional QED. To put it another way, the exact solutions of the one-body Dirac–Coulomb equation (with its negative energy 'pathologies') is equivalent to retaining an arbitrary number of particle–antiparticle pairs in the conventional field-theoretic approach to this problem. This remarkable property of the

Dirac equation does not appear to be widely appreciated. In any case, since the one-fermion Coulomb case has been analysed in detail [2a, 3, 22], as we have outlined, we shall not dwell on it further. Instead, we shall proceed to the two-fermion problem.

3. Two-fermion eigenstates and two-fermion equation

We consider a two-Dirac-fermion state, that is a straightforward generalization of the one-Dirac-fermion state (17), namely

$$|2\rangle = \int \mathrm{d}^3x\, \mathrm{d}^3y\, F_{\alpha\beta}(\boldsymbol{x}, \boldsymbol{y})\psi^\dagger_\alpha(x)\phi^\dagger_\beta(y)|\tilde{0}\rangle \tag{20}$$

where ψ, ϕ could be particle or antiparticle (charge conjugate) fields. We shall be interested in bound states in what follows later, hence we will take one of the fields to be an antiparticle (charge conjugate) field of opposite parity, corresponding to a system like $e^-\mu^+$.

The state (20) is an eigenstate of : H_{CQED} : with eigenenergy E, provided that the 16 coefficient amplitudes $F_{\alpha\beta}(\boldsymbol{x}, \boldsymbol{y})$ satisfy the equations

$$[h_1(\boldsymbol{x})]_{\alpha\gamma}F_{\gamma\beta}(\boldsymbol{x}, \boldsymbol{y}) + [h_2(\boldsymbol{y})]_{\beta\gamma}F_{\alpha\gamma}(\boldsymbol{x}, \boldsymbol{y}) + [V(\boldsymbol{x}, \boldsymbol{y}) - E]F_{\alpha\beta}(\boldsymbol{x}, \boldsymbol{y}) = 0 \tag{21}$$

where

$$V(\boldsymbol{x}, \boldsymbol{y}) = \frac{q_1q_2}{4\pi|\boldsymbol{x} - \boldsymbol{y}|}. \tag{22}$$

In matrix notation, where $F(\boldsymbol{x}, \boldsymbol{y}) = [F_{\alpha\beta}(\boldsymbol{x}, \boldsymbol{y})]$ is a 4×4 'bispinor', equation (21) can be written as

$$[h_1(\boldsymbol{x})]F(\boldsymbol{x}, \boldsymbol{y}) + [h_2(\boldsymbol{y})F^T(\boldsymbol{x}, \boldsymbol{y})]^T + [V(\boldsymbol{x}, \boldsymbol{y}) - E]F(\boldsymbol{x}, \boldsymbol{y}) = 0. \tag{23}$$

Equation (23) is a Dirac-like (or Breit-like) two-fermion Equation. In the absence of the interfermion interaction V, it has solutions of the form

$$F(\boldsymbol{x}, \boldsymbol{y}) = F(\boldsymbol{x})G^T(\boldsymbol{y}) \tag{24}$$

where $F(\boldsymbol{x})$ is a solution of the Dirac equation (19) and $G(\boldsymbol{y})$ is similar to a solution of the Dirac equation

$$(h_2(\boldsymbol{y}) - E_2)G(\boldsymbol{y}) = 0 \tag{25}$$

where $E = E_1 + E_2$.

We note that (21) can be derived by using the variational principle

$$\delta\langle 2| : H_{QED} - E : |2\rangle = 0.$$

This is because, for $\langle\tilde{0}|\boldsymbol{A}|\tilde{0}\rangle = 0$, the trial state $|2\rangle$ is insensitive to the transverse-photon part of the QED Hamiltonian, (7), and so (21) follows directly.

For $|2\rangle$ to be an eigenstate of the momentum operator with eigenvalue $\boldsymbol{P}_{TOTAL} = 0$, it is necessary that the bispinor $F(\boldsymbol{x}, \boldsymbol{y})$ be of the form $F(\boldsymbol{x} - \boldsymbol{y})$, whereupon, in the absence of external classical fields ϕ_c, $\boldsymbol{A}_c$, (23) becomes

$$[h_1(\boldsymbol{r})]F(\boldsymbol{r}) + [h_2(-\boldsymbol{r})F^T(\boldsymbol{r})]^T + [V(r) - E]F(\boldsymbol{r}) = 0 \tag{26}$$

where $\boldsymbol{r} = \boldsymbol{x} - \boldsymbol{y}$ and $V(r) = -\alpha/|\boldsymbol{r}|$ with $\alpha = |q_1q_2|/4\pi$. Equation (26) is a Dirac-like equation for the relative motion of two fermions of masses m_1 and m_2 and charges q_1, q_2 interacting via a Coulomb potential.

It remains, therefore, to solve equation (26) to obtain an exact two-particle Dirac-like eigensolution of the Coulomb QED Hamiltonian. Before reducing the 16 equations (26) we shall consider some limiting cases.

4. Nonrelativistic and one-particle limits of the two-fermion equation

Recalling that in 2×2 block representation

$$h_1(\boldsymbol{r}) = \begin{bmatrix} m_1 & \boldsymbol{\sigma}\cdot\boldsymbol{p} \\ \boldsymbol{\sigma}\cdot\boldsymbol{p} & -m_1 \end{bmatrix} \tag{27}$$

and writing

$$F(\boldsymbol{r}) = \begin{bmatrix} s(\boldsymbol{r}) & t(\boldsymbol{r}) \\ u(\boldsymbol{r}) & v(\boldsymbol{r}) \end{bmatrix} \tag{28}$$

where s, t, u, v are themselves 2×2 matrices, it follows that equation (26) can be written as

$$(m_1 + m_2 + V - E)s - (\boldsymbol{\sigma}\cdot\boldsymbol{p}t^T)^T + \boldsymbol{\sigma}\cdot\boldsymbol{p}u = 0 \tag{29}$$

$$(m_1 - m_2 + V - E)t - (\boldsymbol{\sigma}\cdot\boldsymbol{p}s^T)^T + \boldsymbol{\sigma}\cdot\boldsymbol{p}v = 0 \tag{30}$$

$$(m_2 - m_1 + V - E)u + \boldsymbol{\sigma}\cdot\boldsymbol{p}s - (\boldsymbol{\sigma}\cdot\boldsymbol{p}v^T)^T = 0 \tag{31}$$

$$(-m_1 - m_2 + V - E)v + \boldsymbol{\sigma}\cdot\boldsymbol{p}t - (\boldsymbol{\sigma}\cdot\boldsymbol{p}u^T)^T = 0 \tag{32}$$

where σ_i are the usual Pauli matrices. It is evident (for example, by setting $V = 0$) that (26), or, equivalently, (29)–(32), have, like the Dirac equation, both positive- and negative-energy solutions. Indeed, in this case, there are four kinds: $E \simeq m_1 + m_2$, $E \simeq m_1 - m_2$, $E \simeq -m_1 + m_2$ and $E \simeq -m_1 - m_2$. We shall discuss only the positive-energy solutions, of the type $E \simeq m_1 + m_2$, in this paper.

We note, first, that if we set $E = \epsilon + m_2$ in (29)–(32), then divide through by m_2 and let $m_2 \to \infty$, we obtain the result that $t, v \to 0$ from equations (30) and (32), while the remaining ones reduce to the usual Dirac equations,

$$(m_1 + V - \epsilon)s + \boldsymbol{\sigma}\cdot\boldsymbol{p}u = 0 \tag{33}$$

and

$$(-m_1 + V - \epsilon)u + \boldsymbol{\sigma}\cdot\boldsymbol{p}s = 0. \tag{34}$$

We recall that s and u are 2×2 matrices, so that the Dirac equations (33) and (34) hold for each of the columns of these matrices separately. Similar Dirac equations are obtained in the $m_1 \to \infty$ limit but with s replaced by s^T, u by $-t^T$ and m_1 by m_2 in (33) and (34). Thus the relativistic two-fermion equations (26), or (29)–(32), have Dirac one-particle limits, a property which is held to be desirable for two-fermion equations [10].

For the nonrelativistic limit of the positive-energy solutions we write $E = m_1 + m_2 + \epsilon$ and assume that $|(V - \epsilon)v| \ll |(m_1 + m_2)v|$. Then equation (32) implies that

$$v \simeq \frac{1}{2(m_1 + m_2)}\{\boldsymbol{\sigma}\cdot\boldsymbol{p}t - (\boldsymbol{\sigma}\cdot\boldsymbol{p}u^T)^T\} \tag{35}$$

or, in other words, that v is $\mathrm{O}(\frac{p}{m_i}t, \frac{p}{m_i}u)$. Similarly, therefore, to lowest order in p/m_i, equations (30) and (31) yield the result,

$$t \simeq -\frac{1}{2m_2}(\boldsymbol{\sigma}\cdot\boldsymbol{p}s^T)^T \qquad u \simeq \frac{1}{2m_1}\boldsymbol{\sigma}\cdot\boldsymbol{p}s. \tag{36}$$

Substitution of (36) into (29) shows that, to lowest order in p/m_i, $s(\boldsymbol{r})$ (that is, each of its four components) satisfies the usual Schrödinger equation,

$$\left[\frac{1}{2}\left(\frac{1}{m_1} + \frac{1}{m_2}\right)\boldsymbol{p}^2 + V - \epsilon\right]s(\boldsymbol{r}) = 0 \tag{37}$$

with well known eigenfunctions for $V(r) = -\alpha/r$, and the corresponding eigenvalues $\epsilon_n = -\mu\alpha^2/2n^2$, $\mu = m_1m_2/(m_1 + m_2)$, where $n = 1, 2, 3, \ldots$ is the principal quantum number.

5. J^P eigenstates and radial reduction

If the two-fermion state (20) is to be an eigenstate of J_3 where

$$\boldsymbol{J} = \int \mathrm{d}^3x\, \psi^\dagger(\boldsymbol{x},t)\boldsymbol{j}(\boldsymbol{x})\psi(\boldsymbol{x},t) + \int \mathrm{d}^3x\, \phi^\dagger(\boldsymbol{x},t)\boldsymbol{j}(\boldsymbol{x})\phi(\boldsymbol{x},t) \tag{38}$$

with $\boldsymbol{j}(\boldsymbol{r}) = \boldsymbol{l} + \boldsymbol{s} = -\mathrm{i}\boldsymbol{r}\times\boldsymbol{\nabla} + \frac{1}{2}\boldsymbol{\sigma}$, then we require that the bispinor F (cf (23)) must satisfy the equation

$$j_3(\boldsymbol{r}_1)F(\boldsymbol{r}_1,\boldsymbol{r}_2) + [j_3(\boldsymbol{r}_2)F^T(\boldsymbol{r}_1,\boldsymbol{r}_2)]^T = m_J F(\boldsymbol{r}_1,\boldsymbol{r}_2). \tag{39}$$

In other words, in the frame where $\boldsymbol{P}_{TOTAL}|2\rangle = 0|2\rangle$, and using the notation (28), we require that

$$l_3(\boldsymbol{r})s(\boldsymbol{r}) + \tfrac{1}{2}\sigma_3 s(\boldsymbol{r}) + \tfrac{1}{2}s(\boldsymbol{r})\sigma_3 = m_J s(\boldsymbol{r}) \tag{40}$$

where $\boldsymbol{r} = \boldsymbol{r}_1 - \boldsymbol{r}_2$ and $\boldsymbol{l} = \boldsymbol{r}\times\boldsymbol{p}$. The same equation (40) must be satisfied by the other three components, t, u, v, of the bispinor F. In a similar fashion $\boldsymbol{J}^2|2\rangle = J(J+1)|2\rangle$ implies that the bispinor F in the $\boldsymbol{P}_{TOTAL} = 0$ frame must satisfy the equation

$$(\boldsymbol{l}^2 + \tfrac{3}{2})F + \boldsymbol{l}\cdot\boldsymbol{\sigma}F + (\boldsymbol{l}\cdot\boldsymbol{\sigma}F^T)^T + \tfrac{1}{2}\boldsymbol{\sigma}F\cdot\boldsymbol{\sigma}^T = J(J+1)F \tag{41}$$

and, indeed, since $\boldsymbol{l}^2$ and $\boldsymbol{l}\cdot\boldsymbol{\sigma}$ are block-diagonal, each component, s, t, u, v, of F must satisfy equation (41) individually.

For given J, m_J equations (40) and (41), for any component s, t, u, v of F, have four linearly independent eigensolutions of the form $u(\boldsymbol{r}) = u(r)\varphi(\hat{r})$, etc. We shall denote the 2×2 angular 'bispinor harmonics' by $\varphi^A(\hat{r})$, $\varphi^0(\hat{r})$, $\varphi^+(\hat{r})$, $\varphi^-(\hat{r})$. They are, explicitly ($M \equiv m_J$),

$$\varphi^A(\hat{r}) = \frac{1}{\sqrt{2}}Y_J^M(\hat{r})\begin{bmatrix} 0 & -1 \\ 1 & 0 \end{bmatrix} \tag{42}$$

$$\varphi^0(\hat{r}) = \frac{1}{\sqrt{2J(J+1)}}\begin{bmatrix} \sqrt{(J-M+1)(J+M)}\,Y_J^{M-1} & -MY_J^M \\ -MY_J^M & -\sqrt{(J+M+1)(J-M)}\,Y_J^{M+1} \end{bmatrix} \tag{43}$$

$$\varphi^+(\hat{r}) = \frac{1}{\sqrt{2J(2J-1)}}\begin{bmatrix} \sqrt{(J+M-1)(J+M)}\,Y_{J-1}^{M-1} & \sqrt{(J+M)(J-M)}\,Y_{J-1}^M \\ \sqrt{(J+M)(J-M)}\,Y_{J-1}^M & \sqrt{(J-M-1)(J-M)}\,Y_{J-1}^{M+1} \end{bmatrix} \tag{44}$$

and

$$\varphi^-(\hat{r}) = \frac{1}{\sqrt{2(J+1)(2J+3)}} \times \begin{bmatrix} \sqrt{(J-M+1)(J-M+2)}\,Y_{J+1}^{M-1} & -\sqrt{(J+M+1)(J-M+1)}\,Y_{J+1}^M \\ -\sqrt{(J+M+1)(J-M+1)}\,Y_{J+1}^M & \sqrt{(J+M+1)(J+M+2)}\,Y_{J+1}^{M+1} \end{bmatrix}. \tag{45}$$

We note that φ^A is antisymmetric and $\varphi^{0,\pm}$ are symmetric matrices. Furthermore φ^0, φ^A and $\varphi^\pm$ correspond to opposite parity because $Y_L^M(-\hat{r}) = (-1)^L Y_L^M(\hat{r})$ and φ^0, φ^A have $L = J$ whereas $\varphi^\pm$ have $L = J\pm 1$. These four bispinor harmonics form an orthonormal set, in the sense that $\int \mathrm{d}\hat{r}\ \mathrm{Tr}(\varphi_i^\dagger\varphi_j) = \delta_{ij}$, where $i, j = A, 0, +, -$ and the integrations are taken over the entire solid angle.

Lastly we point out that for the state $|2\rangle$ to be a parity eigenstate, the components s, v, of F must be of opposite parity to that of the components t, u, i.e. if $s(-\boldsymbol{r}) = \pm s(\boldsymbol{r})$ then $t(-\boldsymbol{r}) = \mp t(\boldsymbol{r})$, etc. Taken all together, this means that for a state $|2\rangle$ of a fermion and an

antifermion to be simultaneously an eigenstate of $\boldsymbol{J}^2$, J_3, and parity, the bispinor F, (28), must be of the form

$$F(\boldsymbol{r}) = \frac{1}{r}\begin{bmatrix} \mathrm{i}s_1(r)\varphi^A(\hat{r}) + \mathrm{i}s_2(r)\varphi^0(\hat{r}) & t_1(r)\varphi^-(\hat{r}) + t_2(r)\varphi^+(\hat{r}) \\ u_1(r)\varphi^-(\hat{r}) + u_2(r)\varphi^+(\hat{r}) & \mathrm{i}v_1(r)\varphi^A(\hat{r}) + \mathrm{i}v_2(r)\varphi^0(\hat{r}) \end{bmatrix} \tag{46}$$

for $-(-1)^J$ parity eigenstates, and

$$F(\boldsymbol{r}) = \frac{1}{r}\begin{bmatrix} \mathrm{i}s_1(r)\varphi^-(\hat{r}) + \mathrm{i}s_2(r)\varphi^+(\hat{r}) & t_1(r)\varphi^A(\hat{r}) + t_2(r)\varphi^0(\hat{r}) \\ u_1(r)\varphi^A(\hat{r}) + u_2(r)\varphi^0(\hat{r}) & \mathrm{i}v_1(r)\varphi^-(\hat{r}) + \mathrm{i}v_2(r)\varphi^+(\hat{r}) \end{bmatrix} \tag{47}$$

for $-(-1)^{J\pm1} = (-1)^J$ parity eigenstates. Note that the parity assignments would be interchanged for equations (46) and (47) if $|2\rangle$ were a state of two Dirac particles or two Dirac antiparticles, rather than a Dirac particle–Dirac antiparticle state.

The radial functions in the bispinors (46) and (47) are solutions of the coupled radial equations that are obtained by substituting (46), (47) into (26) (or, equivalently, into (29)–(32)) and equating the coefficients of the four independent bispinor harmonics.

We make use of the following identities in carrying out the radial reduction:

$$\boldsymbol{\sigma}\cdot\boldsymbol{p}f(r)\varphi(\hat{r}) = -\mathrm{i}\frac{\mathrm{d}f}{\mathrm{d}r}\boldsymbol{\sigma}\cdot\hat{r}\varphi(\hat{r}) + \frac{\mathrm{i}}{r}f(r)\boldsymbol{\sigma}\cdot\hat{r}\boldsymbol{\sigma}\cdot\boldsymbol{l}\varphi(\hat{r}) \tag{48}$$

where $\varphi(\hat{r})$ is any 2×2 bispinor harmonic, $f(r)$ a radial function, and $\hat{r} = \boldsymbol{r}/r$, and $\boldsymbol{l} = \boldsymbol{r}\times\boldsymbol{p} = -\mathrm{i}\boldsymbol{r}\times\nabla$. In addition, we note the following useful properties of the above bispinors harmonics:

$$\boldsymbol{\sigma}\cdot\hat{r}\varphi^A = a\varphi^- - b\varphi^+ \tag{49}$$

$$\boldsymbol{\sigma}\cdot\hat{r}\varphi^0 = b\varphi^- + a\varphi^+ \tag{50}$$

$$\boldsymbol{\sigma}\cdot\boldsymbol{l}\varphi^A = f\varphi^0 \tag{51}$$

$$\boldsymbol{\sigma}\cdot\boldsymbol{l}\varphi^0 = -\varphi^0 + f\varphi^A \tag{52}$$

$$\boldsymbol{\sigma}\cdot\boldsymbol{l}\varphi^- = -(J+2)\varphi^- \tag{53}$$

$$\boldsymbol{\sigma}\cdot\boldsymbol{l}\varphi^+ = (J-1)\varphi^+ \tag{54}$$

where

$$a = \sqrt{\frac{J+1}{2J+1}} \qquad b = \sqrt{\frac{J}{2J+1}} \qquad \text{and} \qquad f = \sqrt{J(J+1)}. \tag{55}$$

It is evident from equations (46) and (47) that, in general, eight coupled radial equations are obtained, for arbitrary $J > 0$.

6. Radial equations for the $J = 0$ states and their solution

For the $J = 0$ states, namely the $0^-(^1\mathrm{S}_0)$ and $0^+(^3\mathrm{P}_0)$ states, only two linearly independent bispinor harmonics arise, namely φ^A and φ^- ((42) and(45)), and so $s_2 = t_2 = u_2 = v_2 = 0$ in (46) and (47). (Here, as elsewhere, we give in brackets the nonrelativistic limit designation, $^{2S+1}\mathrm{L}_J$, corresponding to the J^P state in question.) Thus there is only one set of four coupled radial equations for each of $0^-(^1\mathrm{S}_0)$ and $0^+(^3\mathrm{P}_0)$ states:

$$(m_1 + m_2 + V - E)s - t' - \frac{K}{r}t - u' - \frac{K}{r}u = 0 \tag{56}$$

$$(m_1 - m_2 + V - E)t + s' - \frac{K}{r}s + v' - \frac{K}{r}v = 0 \tag{57}$$

$$(m_2 - m_1 + V - E)u + s' - \frac{K}{r}s + v' - \frac{K}{r}v = 0 \tag{58}$$

$$(-m_1 - m_2 + V - E)v - t' - \frac{K}{r}t - u' - \frac{K}{r}u = 0 \tag{59}$$

where $t' = \mathrm{d}t/\mathrm{d}r$, etc, while $K = +1$ for the 0^- and $K = -1$ for the 0^+ states.

If we let $E = m_1 + m_2 + \epsilon$, and assume that $|(V-\epsilon)s| \ll m_i|s|$, etc, in the nonrelativistic limit, then, neglecting also $v \simeq \mathrm{O}(t/m_i, u/m_i)$ in equations (57) and (58), we find that equation (56) reduces to the expected radial Schrödinger equation,

$$(V - \epsilon)s - \frac{1}{2}\left(\frac{1}{m_1} + \frac{1}{m_2}\right)\left(s'' - \frac{K(K-1)}{r^2}s\right) \simeq 0. \tag{60}$$

On the other hand, if we write $E = m_1 + \epsilon$ and let $m_1 \to \infty$, then equations (58) and (59) imply that $u, v \to 0$ while (56) and (57) reduce to the usual radial Dirac equations for s and t. Note that $K = 1$ corresponds to the $J^P = 0^-(^1\mathrm{S}_0)$ states (with $L = S = J = 0$) and $K = -1$ corresponds to the $J^P = 0^+(^3\mathrm{P}_0)$ states (with $L = S = 1, J = 0$) in equations (56)–(59), whereas in the Dirac limit $K = 1$ corresponds to $j + \frac{1}{2}$ with $j = s = \frac{1}{2}$ and $l = 0$ (the $^2\mathrm{s}_{\frac{1}{2}}$ states), while $K = -1$ corresponds to $-(j + \frac{1}{2})$ with $j = s = \frac{1}{2}$, $l = 1$ (the $^2\mathrm{p}_{\frac{1}{2}}$ states). Similarly, if $m_2 \to \infty$, equations (56)–(59) reduce to the radial Dirac equations for s and u, while $t, v \to 0$. In short the coupled radial equations (56)–(59) have the expected nonrelativistic and one-fixed-particle limits.

We have not been able to determine solutions to the coupled radial equations (56)–(59) in terms of common analytic functions. It is of interest, therefore, to consider the properties and general behaviour of the solutions before commencing with numerical solutions.

We anticipate that, as α increases, the eigenenergy spectrum $E(\alpha)$ of equations (56)–(59) will have a qualitative behaviour similar to that of the Dirac spectrum, namely that $E(\alpha)$ decreases monotonically from $E(\alpha = 0) = m_1 + m_2$ until α hits a critical value α_c, beyond which $E(\alpha)$ ceases to be real. It is possible to infer the value of α_c, at least for some cases, by considering the ultra-relativistic limit, $p \to \infty$, in which case we can neglect the masses m_1 and m_2, and seek solutions of (56)–(59) with $E = m_1 = m_2 = 0$. equations (56)–(59) then have the (non-normalizable) solutions $t = u$, $s = v$, $|t| = |s| = 1$ (i.e. $F \propto 1/r$) for $\alpha_c = 2|K| = 2$. Note that this result implies a possible parity degeneracy of α_c. This is analogous to the behaviour of solutions at the critical point of similar momentum-space equations [2, 9, 11–13], for which the momentum-space wavefunction has $E = m = 0$ solutions of the corresponding form $F(p) = 1/p^2$, at $\alpha = \alpha_c$, and for which a parity degeneracy of α_c is observed [11–13]. We might mention that the usual one-particle Dirac–Coulomb equations have a similar $E = m = 0$, $|F| = |G| = 1$ solution at $\alpha_c = |K|$, where F and G are the reduced radial Dirac wavefunctions. These are the correct values of α_c for those states for which $E(\alpha_c) = 0$, and even for those for which $E(\alpha_c) > 0$.

For the Coulomb potential $V = -\alpha/r$, where $\alpha = |q_1 q_2|/4\pi$, it is often convenient to rescale the radial variable, that is to let $\rho = r/a$, where a is a suitable scale parameter. For example, the radial functions s, t, u, v have the large r behaviour $s \sim \mathrm{e}^{-\rho}$, etc, for positive energy $J = 0$ bound states, where a is given by

$$\frac{1}{a^2} = \frac{[(m_1 + m_2)^2 - E^2][E^2 - (m_1 - m_2)^2]}{4E^2} \qquad \underset{m_1 = m_2}{\longrightarrow} m^2 - \left(\frac{E}{2}\right)^2. \tag{61}$$

Note that (61) implies that a is real only for $|m_1 - m_2| \leqslant E \leqslant m_1 + m_2$, which means that the bound state spectrum must lie in this domain. With the rescaling $\rho = r/a$, (56)–(59) become modified slightly, in that r is replaced by $a\rho$ in all of them. For purposes of numerical integration of the radial equations the scale parameter a can be chosen to be anything that is convenient, be it that given in (61), or $a = 1$ or $a = 1/\mu\alpha$, or whatever.

For a power-series analysis of the radial equations it is useful to make the replacement $s = \bar{s}e^{-\rho}$, etc. Assuming solutions of the form

$$\bar{s} = \rho^{\gamma}[a_0 + a_1\rho + a_2\rho^2 + \cdots] \tag{62}$$

$$\bar{t} = \rho^{\gamma}[b_0 + b_1\rho + b_2\rho^2 + \cdots] \tag{63}$$

$$\bar{u} = \rho^{\gamma}[c_0 + c_1\rho + c_2\rho^2 + \cdots] \tag{64}$$

$$\bar{v} = \rho^{\gamma}[d_0 + d_1\rho + d_2\rho^2 + \cdots] \tag{65}$$

we find, upon substitution into the radial equations for $\bar{s}$, $\bar{t}$, $\bar{u}$, $\bar{v}$ and equating coefficients of different powers of ρ, that the following occurs. The coefficients of $\rho^{\gamma-1}$ yield four coupled homogeneous equations for the parameters a_0, b_0, c_0, d_0, which have non-trivial (and non-singular) solutions only if

$$\gamma = \sqrt{K^2 - \left(\frac{\alpha}{2}\right)^2} \tag{66}$$

for any values of m_1, m_2, whereupon

$$\frac{d_0}{a_0} = 1 \qquad \frac{b_0}{a_0}\frac{c_0}{a_0} = -\frac{\alpha}{2(\gamma + K)} = \frac{2(\gamma - K)}{\alpha}. \tag{67}$$

The condition (66) implies that the radial equations have real bound state solutions of the form (62)–(65) only for $\alpha \leqslant 2|K| = 2$, for any values of m_1 and m_2. This, in turn, implies that $\alpha_c \leqslant 2$ for the $0^{\mp}$ states for any values of m_1 and m_2. This condition for bound states, $\alpha \leqslant 2$, is additional to the one that follows from equation (61), namely that $|m_1 - m_2| \leqslant E \leqslant m_1 + m_2$.

The coefficients of the terms in $\rho^{\gamma+\nu}$ yield the recursion relations,

$$a(m_1 + m_2 - E)a_{\nu-1} - \alpha a_\nu - (\gamma + K + \nu)b_\nu + \delta b_{\nu-1} - (\gamma + K + \nu)c_\nu + \delta c_{\nu-1} = 0 \tag{68}$$

$$(\gamma - K + \nu)a_\nu - \delta a_{\nu-1} + a(m_1 - m_2 - E)b_{\nu-1} - \alpha b_\nu + (\gamma - K + \nu)d_\nu - \delta d_{\nu-1} = 0 \tag{69}$$

$$(\gamma - K + \nu)a_\nu - \delta a_{\nu-1} + a(m_2 - m_1 - E)c_{\nu-1} - \alpha c_\nu + (\gamma - K + \nu)d_\nu - \delta d_{\nu-1} = 0 \tag{70}$$

$$(\gamma + K + \nu)b_\nu - \delta b_{\nu-1} + (\gamma + K + \nu)c_\nu - \delta c_{\nu-1} + a(m_1 + m_2 + E)d_{\nu-1} + \alpha d_\nu = 0 \tag{71}$$

where $\delta = 1$. These recursion relations can be used, with (66) and (67) to generate the power series (62)–(65). If $\delta = 0$ then (68)–(71) are the recursion relations for the power series representations of the functions $s(r)$, etc, rather than for $\bar{s}(r)$, etc. Such a series can be used, for example, as a starting procedure for the numerical integration of the radial equations (56)–(59).

Unlike in the Dirac case, the recursion relations (68)–(71) do not admit power series solutions of the form (62)–(65), which terminate at the same power, say $\nu = n'$, so that $a_{n'+1} = b_{n'+1} = c_{n'+1}d_{n'+1} = 0$. In particular, the ground-state solution is not of the simple form

$$\bar{s} = a_0\rho^{\gamma} \qquad \bar{t} = b_0\rho^{\gamma} \qquad \bar{u} = c_0\rho^{\gamma} \qquad \bar{v} = d_0\rho^{\gamma} \tag{72}$$

as it is for the two radial Dirac equations. This is perhaps to be expected, since in the Dirac case there are only two functions, say $\bar{s}$ and $\bar{t}$, and four unknowns to be determined, namely b_0/a_0, γ, a and E. Since the two coupled radial Dirac equations yield four equations (the coefficients of ρ^{γ} and of $\rho^{\gamma-1}$), it is not surprising that a solution is obtained. In the

present case, we have four coupled radial equations (56)–(59), which yield eight equations (the coefficients of ρ^{γ} and of $\rho^{\gamma-1}$) to be satisfied by the six unknowns of the proposed solutions (72), namely b_0, c_0, d_0, γ, a and E. Thus the system is overdetermined and no solution of the form (72) is possible. This situation persists for any solution of the form (62)–(65) where the polynomials all terminate at the same degree. Thus, the radial equations (56)–(59) must be solved numerically.

Before proceeding to do so, we recall that in the conventional QED approach no exact two-fermion eigensolutions of H_{CQED} have been obtained, though perturbative results are available. In analogy to the one-fermion case (section 2) we expect that for small values of α, the eigenvalues $E(\alpha)$ obtained from (56)–(59) should agree with the two-fermion results obtained by the conventional perturbative approach. These conventional perturbative results are [2, 3, 11]:

$$E^{pt}(\alpha) = m_1 + m_2 - \frac{\mu\alpha^2}{2n^2} + \Delta E \tag{73}$$

where $\Delta E = \Delta E_K + \Delta E_C$ is the $O(\alpha^4)$ relativistic correction, made up of corrections to the nonrelativistic kinetic and Coulomb potential energies respectively. The kinetic energy correction has the well known form

$$\Delta E_K = -\frac{1}{2}\alpha^4\mu^4\left(\frac{1}{m_1^3} + \frac{1}{m_2^3}\right)\left(\frac{2}{(2l+1)n^3} - \frac{3}{4n^4}\right). \tag{74}$$

The $O(\alpha^4)$ Coulomb energy correction has been worked out previously for the $J = 0$ and $J = 1$ states [3, 11], and has the form

$$\Delta E_C = -\frac{b\mu^3\alpha^4}{n^3} \tag{75}$$

where

$$b = -\frac{1}{2}\left(\frac{1}{m_1^2} + \frac{1}{m_2^2}\right) \tag{76}$$

for the $0^-(^1S_0)$ states (and for the $1^-(^3S_1)$ states), while

$$b = \frac{1}{6}\left(\frac{1}{m_1^2} + \frac{1}{m_2^2}\right) \tag{77}$$

for the $0^+(^3P_0)$ states.

In comparing our numerical results for the $0^{\mp}$ states with the above $O(\alpha^4)$ results of conventional perturbation theory we find, as is pointed out in more detail below, that they are in agreement when $\alpha \ll 1$ for all values of m_1 and m_2. Indeed, for $\alpha = \frac{1}{137}$, our numerical results are identical to the perturbative ones to at least 12 decimal places for all the values of m_2/m_1 ($0 \leqslant m_2/m_1 \leqslant 1$ in practice) that we tried. To put it another way, the ratio

$$\left[E_{numeric} - \left(m_1 + m_2 - \frac{\mu\alpha^2}{2n^2}\right)\right] \Big/ \Delta E$$

approaches unity with decreasing α, and at $\alpha = \frac{1}{137}$ it deviates from unity by less than 0.001 in all cases that were tried. This emphasizes the fact that the present exact eigenenergies are in agreement with the energies obtained in conventional CQED perturbation theory to at least $O(\alpha^4)$.

For the numerical integration of equations (56)–(59) it is useful to reduce them to a set of two coupled equations by noting that if we subtract equation (59) from (56), we obtain the relation

$$v = -\frac{m_1 + m_2 + V - E}{m_1 + m_2 - V + E}\, s = \frac{\varepsilon + (\alpha/r)}{2(m_1 + m_2) + \varepsilon + (\alpha/r)} s \tag{78}$$

where $V = -\alpha/r$, $E = m_1 + m_2 + \varepsilon$, and $\varepsilon < 0$ for bound states. Similarly, subtracting equation (58) from (57) gives the relation

$$u = \frac{m_1 - m_2 + V - E}{m_2 - m_1 + V - E} t = \frac{2m_2 + \varepsilon + (\alpha/r)}{2m_1 + \varepsilon + (\alpha/r)} t \tag{79}$$

or $u = t$ in the limit of $m_1 = m_2$.

Equation (78) shows that $v(r)$ always has one more node than $s(r)$, namely at $r = -\alpha/\varepsilon$. This again emphasizes that there can be no solutions of the type (62)–(65) which terminate at the same degree for all the radial functions. In the nonrelativistic limit, $\alpha \to 0$, whence $\varepsilon \simeq -\frac{1}{2}\mu\alpha^2$, equation (78) also shows that $v(r)$ is $\mathrm{O}(\alpha^2)s(r)$, that is $v(r)$ is the 'doubly small' component.

Equations (78) and (79) can be used to eliminate u and v from the four radial equations (56)–(59) to yield the two coupled equations

$$\frac{\mathrm{d}s}{\mathrm{d}\rho} = \left[\frac{K}{\rho} + R\right] s + P_t t \tag{80}$$

$$\frac{\mathrm{d}t}{\mathrm{d}\rho} = -\left[\frac{K}{\rho} + Q\right] t + P_s s \tag{81}$$

where

$$R = \frac{(m_1 + m_2)a\alpha}{(\alpha + Ea\rho)([m_1 + m_2 + E]a\rho + \alpha)} \tag{82}$$

$$Q = \frac{(m_2 - m_1)a\alpha}{(\alpha + Ea\rho)([m_1 - m_2 + E]a\rho + \alpha)} \tag{83}$$

$$P_t = \frac{([m_2 - m_1 + E]a\rho + \alpha)([m_1 + m_2 + E]a\rho + \alpha)}{2\rho(Ea\rho + \alpha)} \tag{84}$$

$$P_s = \frac{([m_1 + m_2 - E]a\rho - \alpha)([m_1 - m_2 + E]a\rho + \alpha)}{2\rho(Ea\rho + \alpha)}. \tag{85}$$

We solved equations (80) and (81) numerically using Maple and Fortran Runge–Kutta programs, and the forms (62)–(65) (with $\delta = 0$ in (68)–(71)) as a starting procedure at $\rho \ll \alpha/Ea$ (since α/Ea is the radius of convergence of the power series as is evident from equations (80)–(85)). Some of these numerical results for the lowest-energy $0^{\mp}$ states are listed in tables 1 and 2. Generally, we determined $E(\alpha)$ to four decimal figures, but for particular cases many more decimal figures were determined, as indicated in the tables.

Figure 1 is a plot of E/m versus α for the ground $0^-(n = 1, {}^1\mathrm{S}_0, K = 1)$ and the $0^+(n = 2, {}^3\mathrm{P}_0, K = -1)$ states, in the equal-mass case $m_1 = m_2 = m$. The numerical results are consistent with the critical value $\alpha = 2$, and with the conjectured parity degeneracy of α_c for the $0^{\pm}$ states. We also plot the conventional perturbative results (73), which are seen to follow the numerical results closely for $\alpha \lesssim 1$. Our numerical Maple Runge–Kutta results give $E(\alpha_c = 2) = 0.587\,73$ for the lowest-energy $0^-({}^1\mathrm{S}_0)$ state and $E(\alpha_c = 2) = 1.110\,22$ for the lowest-energy $0^+({}^3\mathrm{P}_0)$ state.

Table 1. $E(\alpha)/m$[a] for the $O^-(1\,^1S_0)$ state, $m_1 = m_2 = m$.

α	$E(\alpha)/m$
0.05	1.999 375 287 8132
0.1	1.997 504 442 0128
0.5	1.939 228 664 1727
0.7	1.8825
0.8	1.8474
0.9	1.8076
1.0	1.762 968 217 2291
1.1	1.7132
1.2	1.6579
1.3	1.5965
1.4	1.5279
1.5	1.450 894 214 1747
1.6	1.3634
1.7	1.2618
1.8	1.1390
1.9	0.9771
1.95	0.8623
1.98	0.7607
2.0	0.587 730 393 6741

[a] $E^{pt}(\alpha)/m = 2 - \frac{1}{4}\alpha^2 + \frac{3}{64}\alpha^4$ in this case.

Table 2. $E(\alpha)/m$ for the $O^+(2\,^3P_0)$ state, $m_1 = m_2 = m$.

α	$E(\alpha)/m$	$E^{pt}(\alpha)/m$
0.5	1.9839	1.9839[a]
0.7	1.9674	1.9676
0.75	1.9623	1.9625
1.0	1.928 55	1.9300
1.25	1.8778	1.8841
1.5	1.7989	
1.7	1.6965	
1.9	1.4989	
1.97	1.3422	
1.99	1.2503	
1.999	1.1564	
2.0	1.110 22	

[a] $E^{pt}(\alpha)/m = 2 - \frac{1}{16}\alpha^2 - \frac{23}{3072}\alpha^4$ in this case.

Figures 2 and 3 are plots of the unnormalized reduced radial wavefunctions $s(r)$, $u(r) = t(r)$ and $v(r) = -[(2m - (\alpha/r) - E]s(r)/[(2m + (\alpha/r) + E]$ in the equal-mass limit, for the lowest-energy $0^-(n = 1\,^1S_0)$ state, when $\alpha = 1$ and $\alpha\alpha_c = 2$ respectively. For $\alpha = 1$ we note that $s(r)$ and $t(r)$ are Dirac-like, with $t(r) \simeq O((\alpha/2)s(r))$ and both functions are nodeless for the ground state. However $v(r)$ does have a node at $r = \alpha/2m - E \simeq 4.22(1/m)$, and $v(r) \simeq O((\alpha/2)^2 s(r))$, that is it is the 'doubly small' component. For $\alpha = \alpha_c = 2$, figure 3 shows that $s(r = 0) = -t(r = 0)$, since $\gamma\sqrt{1 - (\alpha/2)^2} = 0$, as occurs also in the Dirac case. (Recall that for the Dirac case at

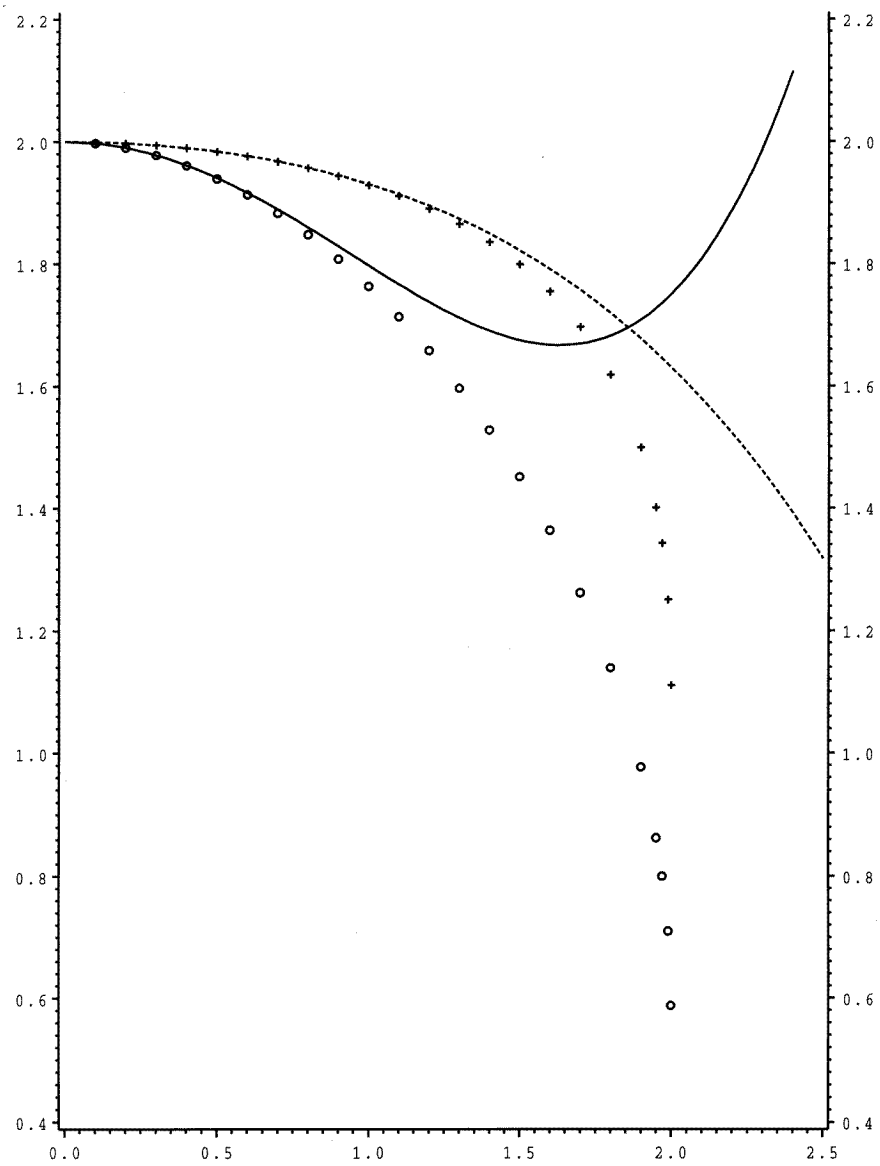

Figure 1. $E(\alpha)/m$ versus α for the equal mass lowest energy $0^-(n = 1\,^1\mathrm{S}_0)$ state (numerical result: open circles; perturbative result: full curve) and $0^+(n = 2\,^3\mathrm{P}_0)$ state (numerical result: plus signs; perturbative result: broken curves) states. $E(\alpha_c = 2)/m = 0.587\,73$ for 0^- and $E(\alpha_c = 2)/m = 1.110\,22$ for 0^+.

$\alpha\alpha_c = 1$, $E = 0$ and $s(r) = -t(r) = \mathrm{e}^{-mr}$ for the ground state.) The single node in $v(r)$ occurs at $r \simeq 1.416(1/m)$ when $\alpha = 2$.

A plot of the reduced radial wavefunctions for the lowest energy $0^+(n = 2\,^3\mathrm{P}_0)$, $K = -1$ state at $\alpha = 1$ is given in figure 4. In this case $s(r)$ is nodeless, but the 'small' component $t(r)$ has one node, as does the 'doubly small' component, $v(r)$. It is straightforward to generate solutions for the $m_1 = m_2$, $0^\pm$ cases for the higher-energy states. One such

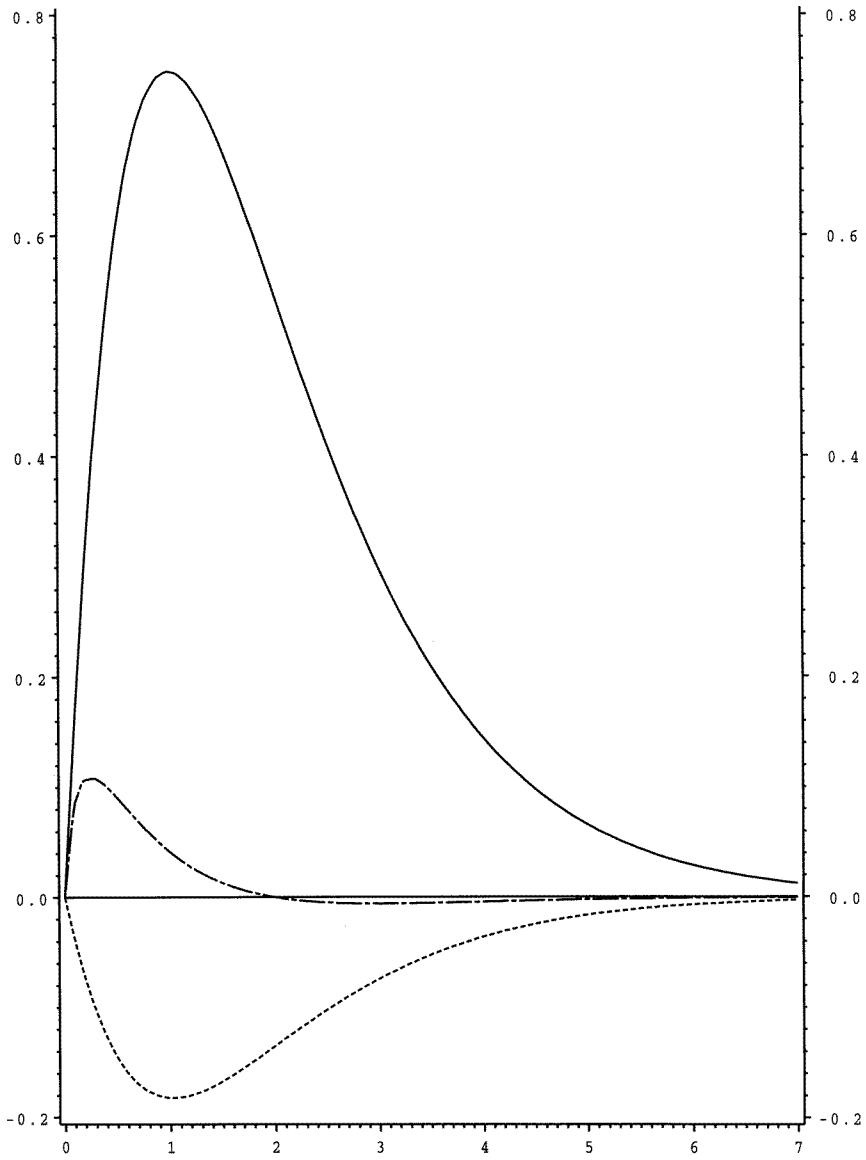

Figure 2. Reduced radial wavefunctions for the $m_1 = m_2 = m$ $0^-(n = 1\,^1S_0)$ ground state for $\alpha = 1$, $E/m = 1.762\,968$. $s(\rho)$: full curve; $t(\rho)$: broken curve; $v(\rho)$: chain curve. $\rho = r/a$, where $a = 2.117\,68(1/m)$.

example, for the first excited $0^+(n = 3\,^3P_0)$ is plotted in figure 5 for the case $\alpha = 2$, for which $E/m = 1.744\,95$. Note that $s(r)$ has two nodes, while $t(r)$ has one and $v(r)$ has three nodes in this case. In addition, $t(r)$ is actually larger than $s(r)$ at this extreme relativistic limit $\alpha = \alpha_c = 2$, where the 0^+ state is quite unlike the nonrelativistic $n = 3\,^3P_0$ state.

The numerical solution of the $m_1 \neq m_2$ cases is equally straightforward, and we computed $E(\alpha)/m_1$ for various mass ratios, among them $m_2/m_1 = \frac{1}{2}, \frac{1}{4}, \frac{1}{10}$, $m_2/m_1 = m_\mu/m_\tau = 0.059\,45\ldots$, $m_2/m_1 = m_e/m_p = 0.000\,544\,617\ldots$, and $m_2/m_1 =$

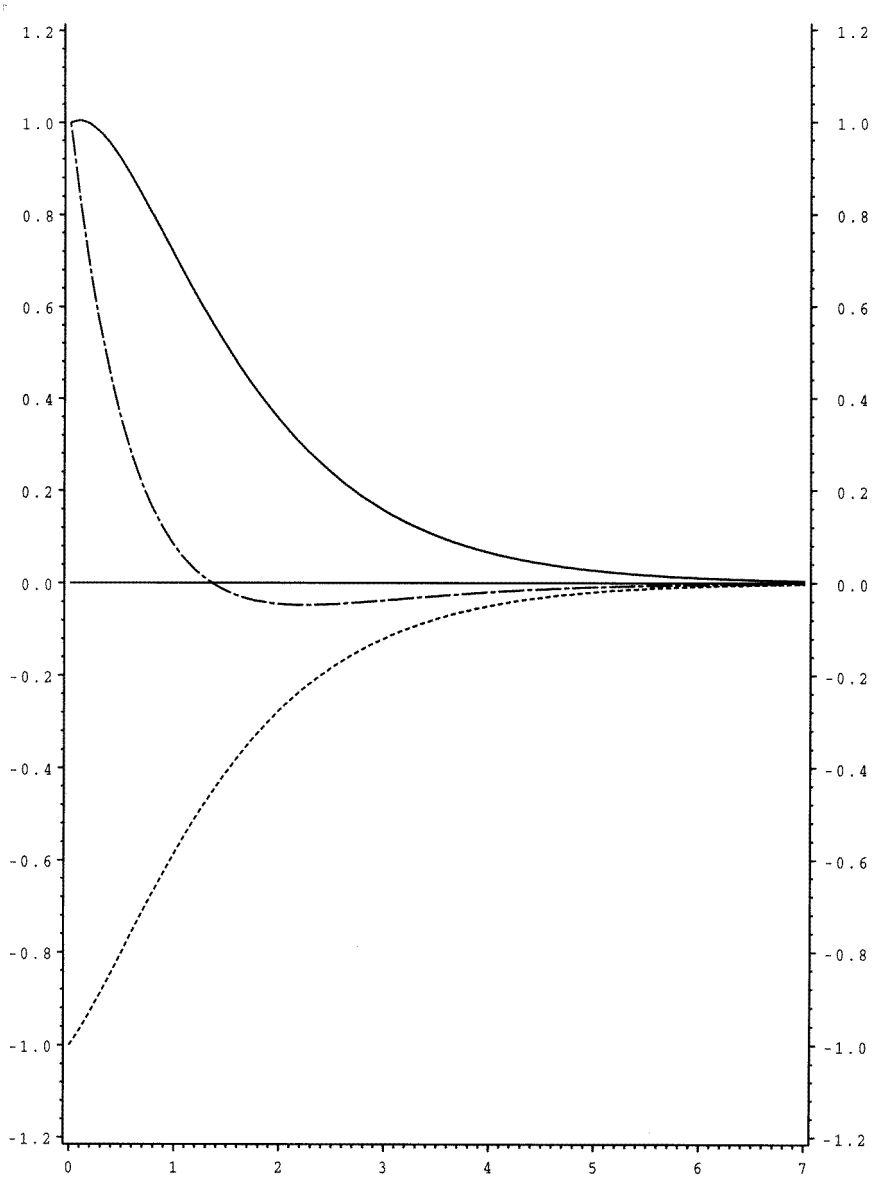

Figure 3. Same as figure 2 but for $\alpha = 2$, $E/m = 0.587\,730$ and $a = 1.046\,19(1/m)$.

$m_e/m(\mathrm{Au}^{197}) = 0.276 \times 10^{-5}$. Some of these numerically determined E/m_1 versus α values are listed in table 3 and plotted in figure 6 for the ground $0^-(^1\mathrm{S}_0)$ case. We do not plot the perturbative results of equation (73) in figure 6 to avoid crowding. In any case the perturbative approximations are virtually indistinguishable from the numerical on this graph for $\alpha \lesssim \alpha_c/2$. Recall that the analysis of the asymptotic behaviour of the bound state $J = 0$ wavefunctions yielded the constraint $|m_1 - m_2| \leqslant E(\alpha) \leqslant m_1 + m_2$ on the mass $M_2 = E(\alpha)$ of the two-body system (61), while the analysis of the small-r behaviour of the wavefunctions yielded the constraint $\alpha \leqslant 2$ (66). Our numerical results are consistent with

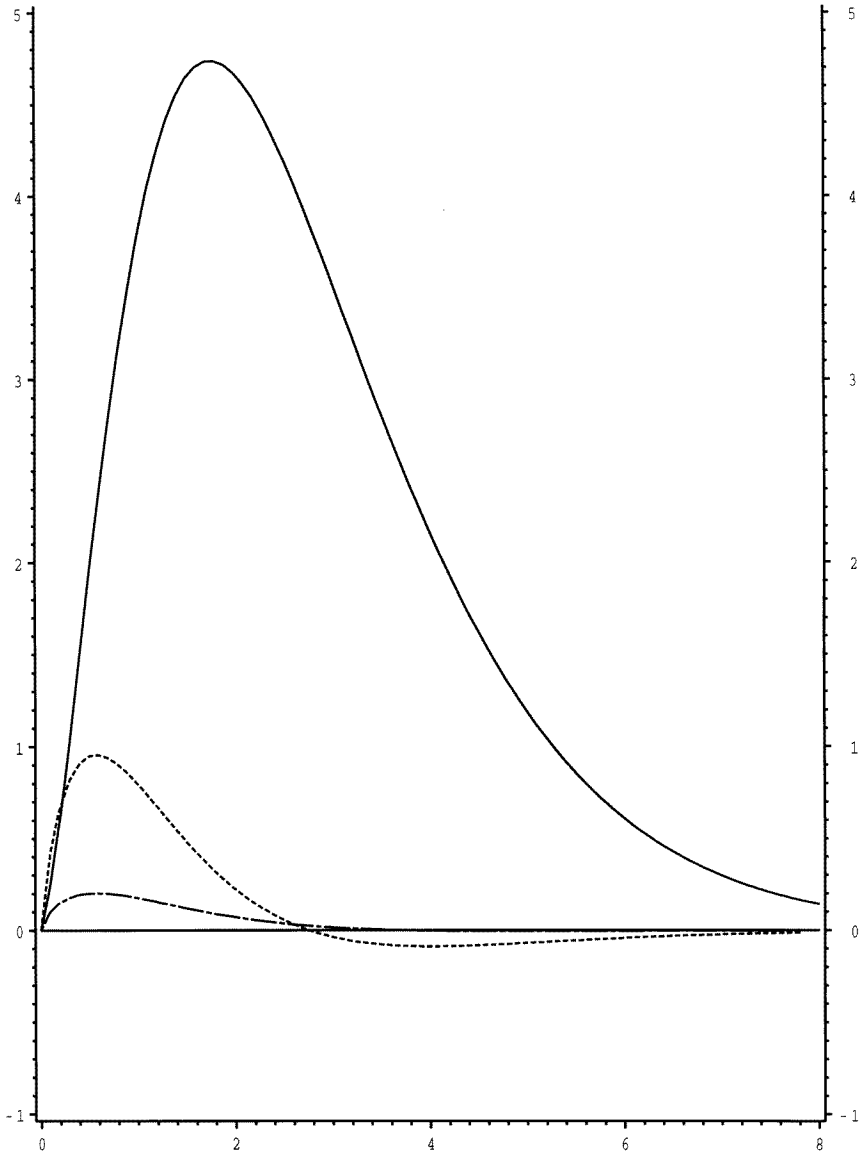

Figure 4. Same as figure 2 but for the lowest energy $0^+(n = 2\,^3P_0)$ state, with $\alpha = 1$, $E/m = 1.928\,55$ and $a = 3.774\,96(1/m)$.

these analytical constraints. Thus, the 0^- radial equations have normalizable ground-state solutions only for $|m_1 - m_2| \leqslant E(\alpha) \leqslant m_1 + m_2$, and for most values of m_2/m_1 the critical values of $\alpha = \alpha_c$ beyond which the solution ceases to be acceptable as representing bound states occur when $E(\alpha_c) = |m_1 - m_2|$. For $E < |m_1 - m_2|$, a becomes imaginary, $a = \mathrm{i}b$, which implies that $s(r)$ behaves as $\mathrm{e}^{-\mathrm{i}br}$. Indeed we find that the numerical solutions do have an oscillatory behaviour for $E < |m_1 - m_2|$. For $m_1 = m_2$ the numerical results indicate that the critical coupling occurs at the other constraint boundary, namely at $\alpha = \alpha_c = 2$, for which $E(\alpha_c) \neq |m_1 - m_2| = 0$ but has the value $E(\alpha_c = 2) = 0.5877$.

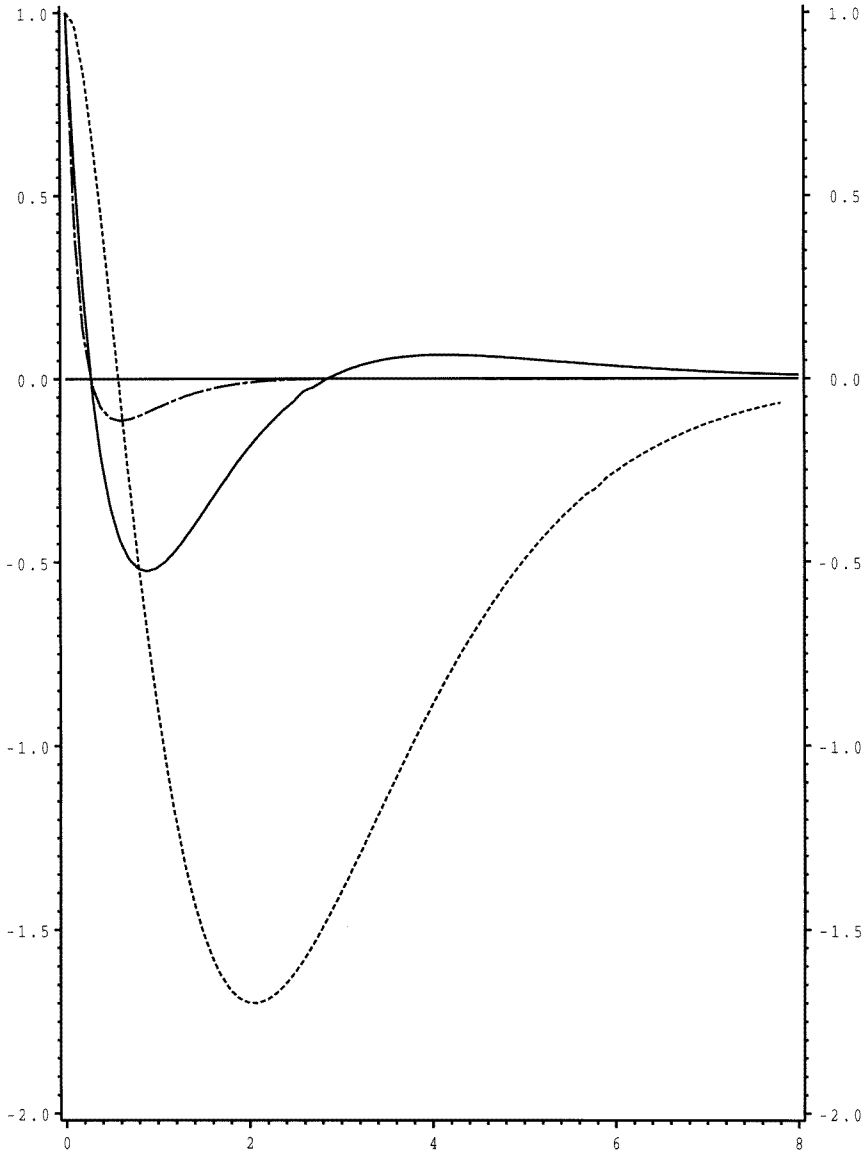

Figure 5. Same as figure 2 but for the first excited $0^+(n = 3\,^3\mathrm{P}_0)$ state, with $\alpha = 2$, $E/m = 1.744\,95$ and $a = 2.046\,417(1/m)$.

Table 4 gives a list of values of α_c for various m_1/m_2 ratios, obtained from the numerical solutions. We note that $\alpha_c = 2$ when $m_1 = m_2$, but decreases towards 1 as $m_1/m_2 \to 0$. This is consistent with the Dirac value of $\alpha_c = 1$. Nevertheless, for real one-electron atoms, the present, higher critical value of $\alpha_c > 1$ ($Z > 137$) is a slight reprieve of the $Z = 137$ Coulomb 'catastrophe' of the Dirac equation, since no nuclei are infinitely heavy. Furthermore, for high-Z one-electron atoms this critical value would be pushed even higher by finite-size effects of the nucleus, as pointed out already for the Dirac case by Greiner and Reinhardt [14].

Table 3. $E(\alpha)/m_2$ for the $0^-(1\,^1S_0)$ state, $m_1 \neq m_2$.

α	$m_1/m_2 = \frac{1}{2}$	$m_1/m_2 = \frac{1}{4}$	$m_1/m_2 = \frac{1}{10}$
0.1	1.498 33	1.2490	1.099 54
0.5	1.459 16	1.2250	1.088 31
0.8	1.3967	1.185 45	1.068 63
1.0	1.3387	1.1477	1.0486
1.2	1.2659	1.0992	1.0212
1.4	1.1752	1.0370	0.983 46
1.6	1.0593	0.9551	0.929 48
1.8	0.8992	0.8376	
1.9	0.782 12		
1.95	0.698 07		
α_c	0.5[a]	0.75[b]	0.9[c]

[a] $\alpha_c = 1.999\,93$.
[b] $\alpha_c = 1.898\,19$.
[c] $\alpha_c = 1.681\,75$.

Table 4. Critical values of α such that $E(\alpha_c) = |m_1 - m_2|$ for the ground state $0^-(^1S_0)$.

$\frac{m_2}{m_1}$	α_c	$\frac{E(\alpha_c)}{m_1} = \left\|1 - \frac{m_2}{m_1}\right\|$
1.0	2.0	0.587 73[a]
0.5	1.999 93	0.5
0.25	1.898 19	0.75
0.1	1.681 75	0.9
$\frac{m_\mu}{m_\tau} = 0.059\,455$	1.571 07	0.940 545
$\frac{m_e}{m_P} = 0.544\,617 \times 10^{-3}$	1.130 04	0.999 455 383
$\frac{m_e}{m(\mathrm{Au}^{197})} = 0.276 \times 10^{-5}$	1.041 870	0.999 997 24

[a] $E(\alpha_c) \neq |m_1 - m_2| = 0$ in this case.

7. Radial equations for $J \geqslant 0$ states

For states with total angular momentum quantum number $J \geqslant 0$ the radial reduction of equations (29)–(32) yields, in general, the eight coupled radial equations

$$(m_1 + m_2 + V - E)s_1 + A\left[-t_1' \mp \frac{J+1}{r}t_1 - u_1' \mp \frac{J+1}{r}u_1\right] + B\left[t_2' - \frac{\tilde{J}}{r}t_2 \pm u_2' \mp \frac{\tilde{J}}{r}u_2\right] = 0 \tag{86}$$

$$(m_1 + m_2 + V - E)s_2 + B\left[t_1' + \frac{\overline{J}}{r}t_1 \mp u_1' \mp \frac{\overline{J}}{r}u_1\right] + A\left[t_2' \mp \frac{J}{r}t_2 - u_2' \pm \frac{J}{r}u_2\right] = 0 \tag{87}$$

$$(m_1 - m_2 + V - E)t_1 + A\left[s_1' \mp \frac{J+1}{r}s_1 + v_1' \mp \frac{J+1}{r}v_1\right] + B\left[-s_2' + \frac{\overline{J}}{r}s_2 \pm v_2' \mp \frac{\overline{J}}{r}v_2\right] = 0 \tag{88}$$

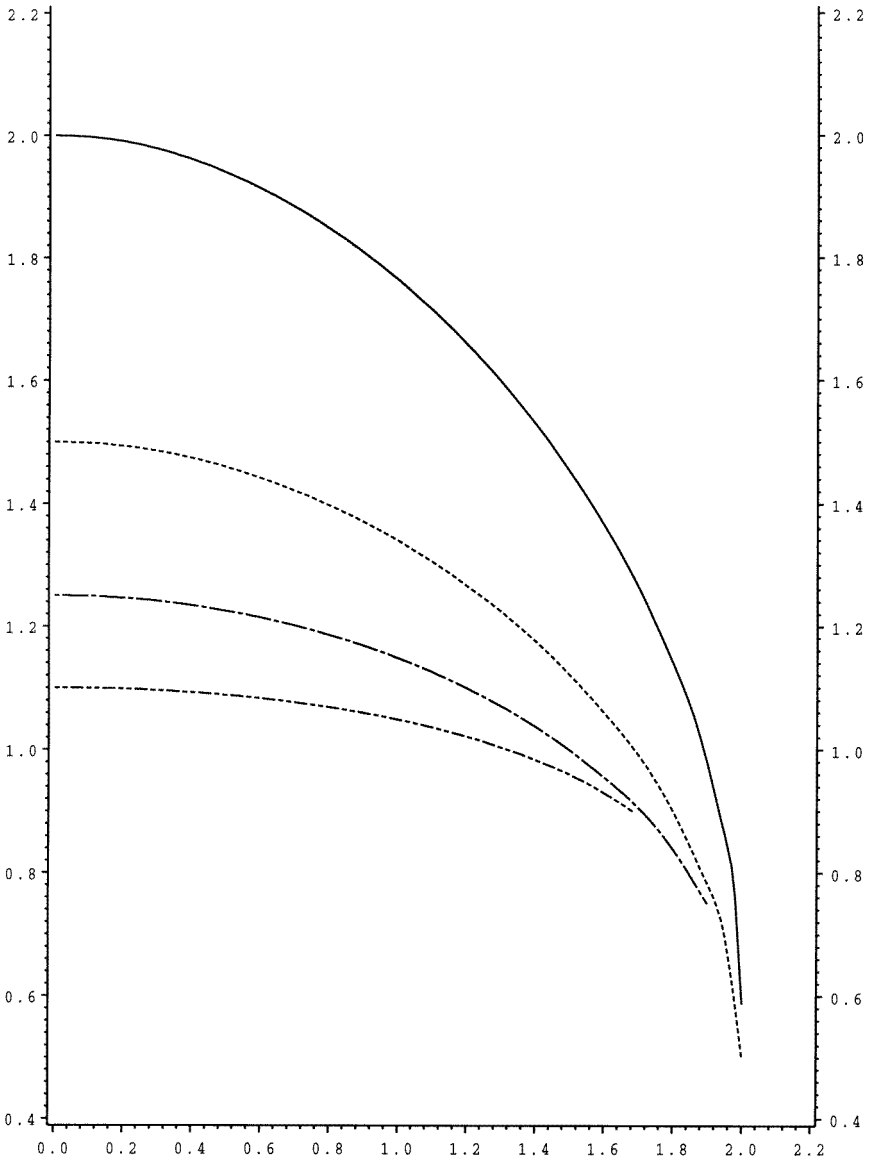

Figure 6. $E(\alpha)/m_1$ versus α for $0^-(n = 1\,{}^1\mathrm{S}_0)$ and various mass ratios: $m_2/m_1 = 1$ (full curve), $\frac{1}{2}$ (broken curve), $\frac{1}{4}$ (chain curve), $\frac{1}{10}$ (dash-double-dot curve).

$$(m_1 - m_2 + V - E)t_2 + B\left[-s_1' - \frac{\tilde{J}}{r}s_1 \mp v_1' \mp \frac{\tilde{J}}{r}v_1\right] + A\left[-s_2' \mp \frac{J}{r}s_2 + v_2' \pm \frac{J}{r}v_2\right] = 0 \tag{89}$$

$$(m_2 - m_1 + V - E)u_1 + A\left[s_1' \mp \frac{J+1}{r}s_1 + v_1' \mp \frac{J+1}{r}v_1\right] + B\left[\pm s_2' \mp \frac{\overline{J}}{r}s_2 - v_2' + \frac{\overline{J}}{r}v_2\right] = 0 \tag{90}$$

$$(m_2 - m_1 + V - E)u_2 + B\left[\mp s_1' \mp \frac{\tilde{J}}{r}s_1 - v_1' - \frac{\tilde{J}}{r}v_1\right] + A\left[s_2' \pm \frac{J}{r}s_2 - v_2' \mp \frac{J}{r}v_2\right] = 0 \tag{91}$$

$$(-m_1 - m_2 + V - E)v_1 + A\left[-t_1' \mp \frac{J+1}{r}t_1 - u_1' \mp \frac{J+1}{r}u_1\right] + B\left[\pm t_2' \mp \frac{\tilde{J}}{r}t_2 + u_2' - \frac{\tilde{J}}{r}u_2\right] = 0 \tag{92}$$

$$(-m_1 - m_2 + V - E)v_2 + B\left[\mp t_1' \mp \frac{\overline{J}}{r}t_1 + u_1' + \frac{\overline{J}}{r}u_1\right] + A\left[-t_2' \pm \frac{J}{r}t_2 + u_2' \mp \frac{J}{r}u_2\right] = 0 \tag{93}$$

where

$$A = \sqrt{\frac{J+1}{2J+1}} \qquad \text{and} \qquad B = \sqrt{\frac{J}{2J+1}}$$

while the upper sign, $\tilde{J} = J$ and $\overline{J} = J + 1$ corresponds to the parity $P = -(-1)^J$ states, and the lower sign, $\tilde{J} = J + 1$ and $\overline{J} = J$ corresponds to the parity $P = (-1)(-1)^{J\pm1}$ states. Note that if $s_2 = u_2 = t_2 = v_2 = 0$ and $J = 0$, then equations (86), (88), (90) and (92) reduce to equations (56)–(59), while the remaining ones vanish identically.

We will not present numerical solutions of the radial equations for $J > 0$ states in this paper, however we shall make a number of observations about them, particularly in the equal mass case.

The $J > 0$ coupled equations (86)–(93) also have the radial Dirac equations as their limit if one of the masses becomes infinite. For example if we let $E = m_1 + \epsilon$, where $m_1 \to \infty$, then equations (90)–(93) imply that u_1, u_2, v_1 and $v_2 \to 0$, whereas (86)–(89) combine and reduce to the two Dirac equations

$$(m_2 + V - \epsilon)G - F' + \frac{\kappa}{r}F = 0 \tag{94}$$

$$(-m_2 + V - \epsilon)F + G' + \frac{\kappa}{r}G = 0 \tag{95}$$

where for the parity $P = -(-1)^J$ (upper sign in (86)–(93)),

$$G = As_1 - Bs_2 \qquad F = t_1$$

with $\kappa = -(J + 1)$, while

$$G = Bs_1 + As_2 \qquad F = -t_2$$

with $\kappa = J$. For the parity $P = -(-1)^{J\pm1}$ (lower sign in (86)–(93)),

$$G = s_1 \qquad F = At_1 - Bt_2$$

for $\kappa = (J + 1)$, and

$$G = s_2 \qquad F = -Bt_1 - At_2$$

for $\kappa = -J$. Equations (86)–(93) reduce similarly to radial Dirac equations in the case $m_2 \to \infty$.

In the nonrelativistic limit, if we set $E = m_1 + m_2 + \epsilon$ and assume that

$$v_i = O\left(\frac{t_i, u_i}{2(m_1 + m_2)}\right) \qquad (i = 1, 2) \tag{96}$$

are negligible, then equations (86)–(93) can be solved for t_i, u_i in terms of s_i, and so eliminated, to yield the expected reduced radial Schrödinger equation for the large component s_i:

$$(V-\epsilon)s_i - \frac{1}{2}\left(\frac{1}{m_1}+\frac{1}{m_2}\right)\left[s_i'' - \frac{l(l+1)}{r^2}s_i\right] = 0 \tag{97}$$

where $l = J$ for both s_1 and s_2 if the parity is $P = -(-1)^J$, but $l = J+1$ for s_1 and $l = J-1$ for s_2 if the parity is $P = -(-1)^{J\pm1}$. In short the radial equations for the $J > 0$ states also have the expected one-fixed-fermion and nonrelativistic limits.

For the Coulomb potential, $V(r) = -\alpha/r$, the critical values of $\alpha = |q_1q_2|/4\pi$, beyond which the radial equations cease to have real solutions, can be inferred for some cases (as also for the $J = 0$ equations, and for the Dirac equation), by considering solutions such that $m_i \to 0$, $E \to 0$, and s_i, t_i, u_i, v_i are constants. It is easily verified that equations (86)–(93) have such solutions for two sets of values of α_c, namely $\alpha_c^2 = 4(J^2+J+1)$ (this includes the $J = 0$ case discussed in section 6) and $\alpha_c^2 = 4J(J+1)$.

The eight radial equations (86)–(93) for $J > 0$ can be reduced to a smaller number in the case of equal masses, $m_1 = m_2 = m$. Thus, for the parity $P = -(-1)^J$ states, they reduce to two sets, one for the singlet ($^1\mathrm{J}_J$) states and one for the triplet ($^3\mathrm{J}_J$) states. For the singlet states $s_2(r) = v_2(r) = 0$, $t_1(r) = u_1(r)$ and $t_2(r) = u_2(r)$, so that equations (86)–(93) become

$$(2m+V-E)s_1 + 2A\left(-t_1' - \frac{J+1}{r}t_1\right) + 2B\left(t_2' - \frac{J}{r}t_2\right) = 0 \tag{98}$$

$$(V-E)t_1 + A\left(s_1' - \frac{J+1}{r}s_1 + v_1' - \frac{J+1}{r}v_1\right) = 0 \tag{99}$$

$$(V-E)t_2 + B\left(-s_1' - \frac{J}{r}s_1 - v_1' - \frac{J}{r}v_1\right) = 0 \tag{100}$$

where

$$v_1(r) = -\frac{2m+V-E}{2m-V+E}s_1(r). \tag{101}$$

For the triplet states, on the other hand, $s_1(r) = v_1(r) = 0$, $u_1(r) = -t_1(r)$, $u_2(r) = -t_2(r)$ and equations (86)–(93) reduce to

$$(2m+V-E)s_2 + 2B\left(t_1' + \frac{J+1}{r}t_1\right) + 2A\left(t_2' - \frac{J}{r}t_2\right) = 0 \tag{102}$$

$$(V-E)t_1 + B\left(-s_2' + \frac{J+1}{r}s_2 + v_2' - \frac{J+1}{r}v_2\right) = 0 \tag{103}$$

$$(V-E)t_2 + A\left(-s_2' - \frac{J}{r}s_2 + v_2' + \frac{J}{r}v_2\right) = 0 \tag{104}$$

where

$$v_2(r) = \frac{2m+V-E}{2m-V+E}s_2(r). \tag{105}$$

For the triplet, parity $P = -(-1)^{J\pm1}$ states, the reduction of the eight coupled radial equations (86)–(93) when $m_1 = m_2$ is not as substantial. Evidently, if $m_1 = m_2$, (88) and (90) imply that $u_1(r) = t_1(r)$, and (89) and (91) imply that $u_2(r) = -t_2(r)$, so that the number of equations is reduced to six. The reason for the relative complexity is the coupling of the $^3(\mathrm{J}+1)_J$ and $^3(\mathrm{J}-1)_J$ states which occurs in this case.

8. Discussion

There are many versions of coordinate-space two-fermion Dirac-like equations with electromagnetic interactions, dating back to the work of Breit [15, 16]. Somewhat surprisingly, the full radial reduction of such equations seems not to have appeared in the literature until 1982, when it was done by Childers [25] in his discussion of the two-body Dirac equation for semirelativistic quarks. Examples of other recent discussions are those of Geiger *et al* [17], Barut and Ünal [18] and Sazdjian [19], and citations therein. The most directly relevant for our purposes are the works of Malenfant [20] and Scott *et al* [21], who deal with Coulomb interactions only (as we do) and who derive coupled radial equations similar to ours. Our approach differs from these works in that we derive the two-fermion equation quantum-field theoretically. Nevertheless, for the equal mass case, which is the only case explicitly considered by these authors, our radial equations are the same as theirs. This is not surprising, since the two-fermion equations considered in both works [20, 21] are sums of free Dirac Hamiltonians with a purely Coulombic interfermion potential, acting on a 16-component wavefunction. They are, in essence, Breit equations with only the Coulomb interaction retained. Thus, the physical content of their equations is the same as that of ours, given that our ansatz (20) is sensitive only to the Coulomb interaction part of the QED Hamiltonian.

Since the formalism and notations are different in these works, we might mention the specific correspondence. Our equal mass, parity $P = -(-1)^J$ singlet state radial equations (97)–(100) are the same as Malenfant's equations ([20], (21)), with the identification $s_1 = P$, $v_1 = R$, $t_1 = -\mathrm{i}Q_+$ and $t_2 = -\mathrm{i}Q_-$, where Malenfant's notation is given on the right. These equations are also the same as Scott *et al*'s equations ([21], (2.10)), with the identification $s_1 = rR_1$, $t_1 = rR_2$, $t_2 = rR_2^*$ and $v_1 = rR_3$, where the Scott *et al* notation is given on the right. For the $P = -(-1)^J$ triplet states our radial equations (101)–(104) are the same as Malenfant's equations ([20], (23)) and Scott *et al*'s equations ([21], (2.12)). The correspondence is $s_2 = P$, $v_2 = R$, $t_1 = -\mathrm{i}Q_+$ and $t_2 = -\mathrm{i}Q_-$ (Malenfant), and $s_2 = rR_1$, $t_1 = -rR_2$, $t_2 = -rR_2^*$ and $v_2 = -rR_3$ (Scott *et al*). There is a similar correspondence among the parity $P = -(-1)^{J\pm1}$ triplet equations.

Malenfant does not give explicit numerical solutions in his paper [20], while Scott *et al* [21] give results for $m_1 = m_2$ and $\alpha = \frac{1}{137}$ only. They quote energy eigenvalues $E(\alpha = \frac{1}{137})$ to 18 decimal figures, for $n = 1, 2, 3$ $^{2S+1}\mathrm{L}_J$ states (in the nonrelativistic designation), which they obtained using the finite element method. In our Runge–Kutta calculations we have generally retained not more than 14 significant figures. However, as a check we calculated the ground-state energy to 18 figures and obtained the identical result as Scott *et al* [21], namely $E_{gr}/m = 1.999\,986\,680\,297\,077\,760$.

For $\alpha \ll 1$ the numerical two-fermion Coulomb QED energy eigenvalues when $m_1 = m_2$ are in excellent agreement with conventional perturbative results (73), $\Delta E = \Delta E_K + \Delta E_C$, with

$$\Delta E_K = -\frac{1}{16} m\alpha^4 \left(\frac{2}{(2l+1)n^3} - \frac{3}{4n^4} \right) \tag{106}$$

and

$$\Delta E_C = -\frac{1}{8} bm\alpha^4 \frac{1}{n^3} \tag{107}$$

where $b = -1$ for the $0^{-+}(^1\mathrm{S}_0)$ and $1^{--}(^3\mathrm{P}_1)$ states, $b = \frac{1}{3}$ for $0^{++}(^3\mathrm{P}_0)$, $b = \frac{1}{6}$ for

$1^{++}(^3\mathrm{P}_1)$ and $b = 0$ for the $1^{+-}(^1\mathrm{P}_1)$ states. Equations (105) and (106) yield

$$\frac{\Delta E}{m\alpha^4} = \frac{3}{64}, -\frac{23}{3072}, -\frac{5}{1024}, -\frac{7}{3072}$$

for the $0^{-+}(1\,^1\mathrm{S}_0)$, $0^{++}(2\,^3\mathrm{P}_0)$, $1^{++}(2\,^3\mathrm{P}_1)$ and $1^{+-}(2\,^1\mathrm{P}_1)$ states respectively. Note that for an $m_1 = m_2$ particle–antiparticle system the states are also charge conjugation eigenstates, hence we have given their J^{PC} designations above.

Thus, for the ground state, the conventional perturbative result from equations (105) and (106) is $E_{gr}^{pt}/m = 1.999\,986\,680\,297\,163\,899\ldots$, which is the same as the numerical result to 12 decimal figures. Indeed, at this low value of $\alpha = \frac{1}{137}$, the numerical energy eigenvalues agree with the perturbative values to an increasingly larger number of decimal figures for the higher-energy states. For example, Scott *et al* [20] give $E(n = 2\,^3\mathrm{P}_0)/m = 1.999\,996\,670\,019\,771\,708$, as compared to the perturbative result ((105) and (106)) of $E^{pt}(n = 2\,^3\mathrm{P}_0)/m = 1.999\,996\,670\,019\,771\,893\ldots$. These are identical to 15 decimal figures. In the case of the $n = 2\,^3\mathrm{P}_1$ state the numerical and perturbative results differ by one in the eighteenth decimal figure.

In comparing our two-fermion Dirac-like equation results (in which the negative-energy components are retained and the vacuum is empty) to the lowest-order conventional Coulomb QED results [3, 11] (in which the negative-energy components are effectively projected out, and the vacuum is a Dirac 'filled negative-energy sea'), we note the following. The results are very similar at low α (indeed the energy eigenvalues are the same to $\mathrm{O}(\alpha^4)$), but they are rather different for higher α. The difference in the highly relativistic limit can be seen very clearly by comparing the critical values of α. In the equal mass case, the lowest energy $\mathrm{O}^{\mp}$ states have $\alpha_c = 2$ in the present formalism, but $\alpha_c = 8\pi/(4+\pi^2) = 1.812\ldots$ in the lowest-order conventional formalism [11]. The disagreement at high α is, we believe, due to the severe truncation of the infinite chain of Fock states that has been done in the quoted conventional CQED studies. In analogy to what happens in the one-fermion ($m_1/m_2 \to 0$) limit, we expect that the two set of results would be the same if it were possible to keep all orders in the conventional approach.

We do not compare the present results to the observed spectra of systems such as $\mu^+\mathrm{e}^-$ and $\mathrm{e}^+\mathrm{e}^-$ since we have dealt here only with part of the QED Hamiltonian (the static Coulomb part). The inclusion of transverse photon effects, which have been neglected in this work, is a straightforward matter, at least at the perturbative $\mathrm{O}(\alpha^4)$ level in the conventional approach [11, 13]. This then brings the predicted energy levels into $O(\alpha^4)$ agreement with the observed spectra for systems such as $\mu^+\mathrm{e}^-$ and $\mathrm{e}^+\mathrm{e}^-$ [4–8, 25]. However, the inclusion of the transverse photon interaction (7) in a non-perturbative, rigorously variational way remains an outstanding problem.

Finally, we point out that the generalization of the present formalism to a three-fermion Dirac-like system with purely Coulombic interactions, is straightforward, at least in principle. It is only necessary to replace the two-particle ansatz (20) with a three-particle one [23, 24]:

$$|3\rangle = \int \mathrm{d}^3x\,\mathrm{d}^3y\,\mathrm{d}^3z\; F_{\alpha\beta\gamma}(\boldsymbol{x}, \boldsymbol{y}, \boldsymbol{z})\psi_\alpha^\dagger(x)\psi_\beta^\dagger(y)\phi_\beta^\dagger(z)|\tilde{0}\rangle \tag{108}$$

Of course, the reduction of the resulting system of equations to radial form is much more complicated, and even then one is left with the full complexity of a three-body problem.

9. Summary

We have shown that the Coulomb QED Hamiltonian has exact Dirac-like few-particle eigenstates, which are just the usual Dirac states in the one-body case. In the case of two bodies, the states are described by a 4×4 matrix Breit-like equation, with purely Coulombic interfermion interactions. The two-fermion equation has the usual Dirac equation as its one particle limit (when one of the fermion masses is infinite). It has the Schrödinger equation for the relative motion of the two particles as its nonrelativistic limit.

We determined the form of the 4×4 eigenmatrices for specific J^P states. This led to a simple and straightforward radial reduction of the two-fermion matrix equation. The resulting radial equations have the radial Dirac equations as their one-body limit. These radial equations are also shown to be equivalent to other radial reductions of two-fermion equations with purely Coulombic interactions [20, 21].

We solved the radial equations numerically for a number of $J^P = 0^{\pm}$ states, for various combinations of the masses, m_1 and m_2 of the two fermions, and various strengths of the coupling $\alpha = |q_1q_2|/4\pi$, where q_1 and q_2 are the charges of the two fermions. For low α our numerical solutions for the eigenenergies are in agreement with previously obtained $O(\alpha^4)$ conventional perturbative solutions [3, 11]. Our numerical results also agree with the only other accurate numerical results that we know of, namely those of Scott *et al* [21], who have published solutions for the equal mass case, $m_1 = m_2$, for $\alpha = \frac{1}{137}$.

Our numerical results for the energy eigenvalues as a function of α, $E(\alpha)$, for various values of the ratios m_1/m_2, show that $E(\alpha)$ has a Dirac-like behaviour. That is, $E(\alpha)$ starts out with the non-relativistic form $m_1 + m_2 - \mu\alpha^2/2n^2$ for $\alpha \to 0$ and then decreases monotonically to $E(\alpha_c) \geqslant |m_1 - m_2|$ as α reaches a critical value α_c. We find that $\alpha_c = 2$ for $m_1/m_2 = 1$ but decreases monotonically with decreasing m_1/m_2 to the Dirac-Coulomb value $\alpha_c = 1$ as $m_1/m_2 \to 0$. The results that $\alpha_c \leqslant 2$ and $E \geqslant |m_1 - m_2|$ are also obtained analytically from an analysis of the small-r and asymptotic behaviour of the radial wavefunctions (cf (66) and (61)). Lastly, our numerical results indicate a parity degeneracy of $\alpha_c = 2$ when $m_1 = m_2$ for the 0^- and 0^+ states (which start off, at low α, as $^1S_0$ and $^3P_0$ states respectively).

Acknowledgments

The financial support of the Natural Sciences and Engineering Research Council of Canada for this work is gratefully acknowledged. JWD would like to thank the Fondation Louis de Broglie in Paris, where part of this work was done, for their hospitality.

References

[1] Bjorken J D and Drell S D 1965 *Relativistic Quantum Fields* (New York: McGraw-Hill)
[2] Hardekopf G and Sucher J 1984 *Phys. Rev.* A **30** 703; 1985 *Phys. Rev.* A **31** 2020
[3] Darewych J W and Horbatsch M 1989 *J. Phys. B: At. Mol. Opt. Phys.* **22** 973
[4] Ferrell R A 1951 *Phys. Rev.* **84** 858
[5] Rich A 1981 *Rev. Mod. Phys.* **53** 127
[6] Lepage G P 1977 *Phys. Rev.* A **16** 863
[7] Bowdin G F and Yennie D R 1978 *Phys. Rep.* **43C** 267
[8] Bowdin G F, Yennie D R and Gregorio M A 1982 *Phys. Rev. Lett.* **48** 1799
[9] Finger J, Horn D and Mandula J E 1979 *Phys. Rev.* D **20** 3253
[10] Gross F 1982 *Phys. Rev.* C **26** 2203
[11] Darewych J W and Horbatsch M 1990 *J. Phys. B: At. Mol. Opt. Phys.* **23** 337

[12] Hersbach H 1992 *Phys. Rev.* A **46** 3657
[13] Dykshoorn W and Koniuk R 1990 *Phys. Rev.* A **41** 64
[14] Greiner W and Reinhardt J 1992 *Quantum Electrodynamics* (New York: Springer) ch 7
[15] Breit G 1929 *Phys. Rev.* **51** 248
[16] Bethe H A and Salpeter E E 1957 *Quantum Mechanics of One and Two Electron Atoms* (New York: Springer)
[17] Geiger K, Reinhardt J, Müller B and Greiner W 1988 *Z. Phys.* A **329** 77
[18] Barut A O and Ünal N 1986 *J. Math. Phys.* **27** 3055
[19] Sazdjian H 1989 *Ann. Phys.* **191** 52
[20] Malenfant J 1988 *Phys. Rev.* D **38** 3295
[21] Scott T C, Shertzer J and Moore R A 1992 *Phys. Rev.* A **45** 4393
[22] Guiasu I and Koniuk R 1993 *Can. J. Phys.* **71** 360
[23] Berseth W C and Darewych J W 1993 *Phys. Lett.* **178A** 347 (1994 erratum *Phys. Lett.* **185** 503)
[24] Di Leo L and Darewych J W 1993 *Can. J. Phys.* **71** 365
[25] Childers R W 1982 *Phys. Rev.* D **26** 2902